pISSN 1229-3008 eISSN 2287-6251
Progress in Superconductivity and Cryogenics
Vol. 26, No. 4, (2024), pp.41~45 https://doi.org/10.9714/psac.2024.26.4.041

A preliminary cost analysis for superconducting magnetic energy storage (SMES) using HTS REBCO tape

Dongsu Seo[a], Chaemin Im[b], Jaheum Koo[a], EunSeok Yang[c], Seungyong Hahn[*, a], and Sangjin Lee[a]

[a] *Department of Electrical and Computer Engineering, Seoul National University, Seoul, 08826, Korea*
[b] *Applied Superconductivity Center, Seoul National University, Seoul, 08826, Korea*
[c] *Department of Future Automotive Mobility, Seoul National University, Seoul, 08826, Korea*

(Received 6 December 2024; revised or reviewed 24 December 2024; accepted 25 December 2024)

Abstract

This research presents a preliminary cost analysis and estimation for superconductor used in superconducting magnetic energy storage (SMES) systems, targeting energy capacities ranging from 1 MJ to 1 GJ, relevant for power grid and industrial applications. Utilizing high-temperature superconductor (HTS) rare-earth barium copper oxide (REBCO) coils in SMES can help compensate for power quality degradation and enhance power stability. However, the high capital costs of SMES remain significant challenges, with costs varying across different energy capacities. First, SMES designs in solenoidal configurations are presented and compared, considering design parameters such as total conductor length, operating current, and magnetic field at the coil center. Then, preliminary cost estimates of these designs are provided based on the price of superconductor. This analysis offers insights into the economic considerations for superconductor in SMES designs and highlights the potential benefits of implementing HTS REBCO-based SMES systems across various applications.

Keywords: superconducting magnetic energy storage (SMES), HTS, REBCO, cost analysis, energy storage system (ESS)

1. INTRODUCTION

As global energy systems increasingly rely on renewable energy to meet the growing demand for low-carbon, green growth, the need for reliable and efficient energy storage systems (ESS) has become more significant. ESS plays a crucial role in balancing energy supply and demand, improving power quality, and maintaining grid stability [1]. Researchers have been investigating superconducting magnetic energy storage (SMES) systems as a potential solution for ensuring steady power quality and energy reliability. In addition, SMES compensates for energy loss caused by the unpredictable and intermittent behavior of renewable energy sources [2].

Unlike conventional energy storage systems, SMES stores energy as a magnetic field using superconducting coils configured in solenoidal and toroidal topologies. It is expected to offer advantages such as high cyclic efficiency and highly efficient energy storage [3], while helping to stabilize power quality and mitigate energy fluctuations through frequency regulation [4].

Recent advancements and extensive research on high-temperature superconductors (HTS), particularly rare-earth barium copper oxide (REBCO), have demonstrated their potential to enhance the performance of SMES systems. While applying REBCO to SMES systems is expected to improve performance characteristics, such as higher critical current density and enhanced stability under strong magnetic fields, a comprehensive economic cost analysis is essential to effectively implement HTS REBCO SMES systems.

Compared to low-temperature superconductors (LTS), first, HTS operates at higher temperatures, providing a more cost-effective and efficient operational environment. Thus, HTS SMES is expected to outperform LTS SMES in terms of overall performance and reliability.

Second, HTS can operate at relatively higher temperatures than low-temperature superconductors (LTS) by using cost-effective liquid nitrogen instead of liquid helium [5]. This not only reduces cooling costs but also enables improved thermal stability and operational efficiency at these temperatures, making HTS SMES more robust and practical than LTS SMES. Furthermore, REBCO stands out for its peak magnetic field > 20 tesla [6] in large-scale applications.

The capital costs of SMES include superconducting materials, cryogenic control systems, power conditioning systems [7], and other infrastructure costs for integration into external power grids. Among these, the extensive use of superconducting tape is one of the hindrances to the widespread commercialization of SMES.

This paper presents a preliminary cost analysis of superconductor used in SMES design, focusing on energy capacities of 1 MJ to 1 GJ. This energy range is selected to meet the demands of load leveling and power stabilization in power systems, where short-term high-power output is essential for grid stability. It also supports the energy needs of industrial machinery, such as large-scale motors, making SMES ideal for industries. By focusing on this range, the research addresses the operational and economic

* Corresponding author: hahnsy@snu.ac.kr

needs of both power systems and industrial applications.

Key design parameters, such as total conductor length, operating current, and center magnetic field in a solenoidal coil, are analyzed and compared. The commercial price of superconducting tape is applied to estimate the cost trend for these energy capacities. Through this cost analysis, the study offers economic insights into HTS SMES design for the power and industrial sectors.

2. HTS SMES TOPOLOGY DESIGN

2.1. Design Requirements and Constraints

The design requirements are as follows: 1) The HTS tape used is 4 mm × 140 μm GdBCO ($GdBa_2Cu_3O_{7-\delta}$) tape fabricated by SuNAM Co., Ltd., with gadolinium as the rare-earth element; 2) The operating temperature is fixed at 20 K, enabling helium-free conduction cooling, which affects the critical current of the SMES coil; 3) To ensure reliable operation, the operating current must remain within a 30 % margin of the critical current [8], as derived from the critical current data of the GdBCO tape at 20 K; 4) The hoop stress, a circumferential stress caused by the radial component of Lorentz force along the coil's winding path, must be limited to below 400 MPa [9, 10]. By complying with these requirements, the final design aims to achieve energy capacities ranging from 1 MJ to 1 GJ with the minimum conductor length.

To minimize conductor usage, a parametric sweep is employed to explore design parameters within the given input ranges of inner radius, number of turns, and number of double pancake coils. Among the results, the model with the lowest stress was selected as the most suitable parameter.

To ensure that the hoop stress remains below 400 MPa for each energy level, stainless steel co-winding with varying thicknesses is applied, effectively reducing the hoop stress to meet the design requirements. The hoop stress is calculated using the *BJR* hoop stress formula [11], which approximates the hoop stress in a single turn under a magnetic field. The designed SMES in solenoidal configuration is treated as a whole body to estimate the approximate hoop stress. In this formula, *B* represents the magnetic field at the outermost middle line of the solenoid, *J* represents the current density, and *R* represents the inner radius [12]. The *BJR* hoop stress (2) is derived from the force balance equation [13], where σ_r is the radial stress and *r* is the inner radius, as shown in (1).

$$r\frac{\partial \sigma_r}{\partial r} + \sigma_r - \sigma_h + rJ(r)B(r) = 0 \tag{1}$$

$$\sigma_h = BJR \tag{2}$$

2.2. Design with Finite Element Method

The parametric design of HTS SMES coils for energy capacities ranging from 1 MJ to 1 GJ is conducted using the finite element analysis software COMSOL Multiphysics. The parameters required to achieve each target energy capacity are determined using a parametric sweep in the software, as described previously.

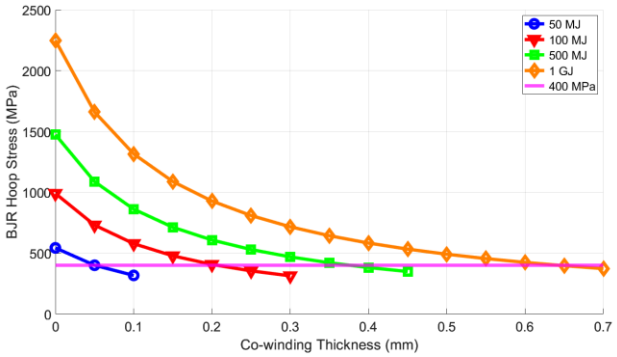

Fig. 1. Variation of *BJR* hoop stress with respect to stainless steel co-winding thickness.

To achieve the target stored energy values while satisfying the design requirements, parameters such as the inner radius of the coil, the number of turns, the number of double pancake coils, and the operating current are considered. These parameters directly affect the stored energy for the SMES. The equation for the stored energy is provided in (3), where *E* represents the total energy stored in the SMES, *L* represents the inductance determined by the solenoidal configuration of the SMES coil, and I_{op} represents the operating current flowing through the SMES coil [14].

$$E = \frac{1}{2}LI_{op}^{\ 2} \tag{3}$$

The inductance (*L*) is calculated using the energy method. The total stored energy (*E*) is obtained through finite element method (FEM) simulations, and the inductance is derived as shown in (4).

$$L = \frac{2E}{I_{op}^{\ 2}} \tag{4}$$

2.3. Design Specifications from 1 MJ to 1 GJ

The energy capacities are subdivided into 1 MJ, 5 MJ, 10 MJ, 50 MJ, 100 MJ, 500 MJ, and 1 GJ. Fig. 1 illustrates the relationship between stainless steel co-winding thickness and *BJR* hoop stress, with co-winding thicknesses of 0.10 mm, 0.25 mm, 0.40 mm, and 0.65 mm applied to energy capacities of 50 MJ, 100 MJ, 500 MJ, and 1 GJ, respectively. These thicknesses represent the minimum required to ensure *BJR* hoop stress remains below 400 MPa. Energy capacities of 1 MJ, 5 MJ, and 10 MJ are excluded from the analysis because their *BJR* hoop stress naturally remains below 400 MPa without additional co-winding.

In Fig. 1, each colored curve represents the energy capacities: blue circles for 50 MJ, red triangles for 100 MJ, green squares for 500 MJ, and orange diamonds for 1 GJ. As the co-winding thickness increases, the *BJR* hoop stress for each energy capacity gradually decreases, falling below the 400 MPa threshold, represented by the magenta line. The final co-winding thicknesses of 0.10 mm, 0.25 mm, 0.40 mm, and 0.65 mm correspond to *BJR* hoop stresses of 318.6 MPa, 355.8 MPa, 383.2 MPa, and 398.2 MPa, respectively. Thus, the *BJR* hoop stress for each energy

TABLE I
HTS SMES DESIGN SPECIFICATIONS FROM 1 MJ TO 1 GJ.

Parameters	Units	1 MJ	5 MJ	10 MJ	50 MJ	100 MJ	500 MJ	1 GJ
Width	[mm]	4.1	4.1	4.1	4.1	4.1	4.1	4.1
Thickness (REBCO + co-wound)	[mm]	0.14	0.14	0.14	0.14 + 0.10	0.14 + 0.25	0.14 + 0.40	0.14 + 0.65
Single pancake height	[mm]	0.2	0.2	0.2	0.2	0.2	0.2	0.2
Double pancake height	[mm]	0.6	0.6	0.6	0.6	0.6	0.6	0.6
Inner diameter	[mm]	300	600	800	1,200	2,400	3,400	5,400
Outer diameter	[mm]	342	642	845	1,294	2,551	3,619	5,708
Coil height	[mm]	1,637.4	2,249.4	2,429.4	4,013.4	2,483.4	5,399.4	4,931.4
Number of turns	[-]	150	150	160	196	193	203	195
Number of DP	[-]	182	250	270	446	276	600	548
Total conductor length	[km]	55.1	146.3	223.2	684.9	828.5	2,685.9	3,729.1
Critical current	[A]	158.9	157.4	153.0	141.7	148.3	143.6	149.9
Operating current	[A]	111	110	107	100	104	100	105
Current density	[A/mm²]	193.4	191.6	186.4	101.6	65.0	45.2	32.4
Volumetric energy density	[MJ/m³]	8.7	7.9	8.2	11.0	8.9	10.3	8.9
Stored energy	[MJ]	1	5	10	50	100	500	1,000
Total inductance	[H]	162.8	828.1	1,748.6	10,000	18,502	100,767	181,635
Center field (Bz)	[T]	4.6	4.4	4.5	5.2	4.0	4.8	3.8
BJR hoop stress	[MPa]	130.9	253.1	336.0	318.6	355.8	383.2	398.2

capacity is effectively reduced below 400 MPa.

Table I presents the design parameters categorized by the energy capacities of the SMES coil, ranging from 1 MJ to 1 GJ. The classification is focused on design parameters, including operating current, total inductance, conductor length, and current density, which collectively determine the coil's stored energy and structural stability. The total conductor length scales proportionally with energy capacities, while current density decreases to maintain thermal and electromagnetic stability. Additionally, co-winding thickness is introduced to ensure the stress level remains below the structural limit of 400 MPa. This classification highlights the balance between maximizing stored energy and ensuring mechanical stability in SMES coil design.

Fig. 2 illustrates the geometric design of SMES coil, including key parameters such as the inner radius (a_1), outer radius (a_2), coil height (b), and the number of turns (N_{Turns}). The parameters b and N_{Turns} are calculated by considering the width and thickness of the HTS tape.

For high-capacity SMES designs, such as the 1 GJ SMES, the inductance becomes significantly large. While quick energy discharge is generally a feature of insulated SMES coil, the no-insulation (NI) coil with stainless steel co-winding designed in this research exhibits charge-discharge delay behavior [15]. In an NI coil's equivalent circuit, the characteristic resistance (R_c) remains constant, while the inductance varies. Consequently, the large inductance in high-capacity SMES designs leads to an increased time constant ($\tau = L/R_c$), resulting in delayed energy discharge.

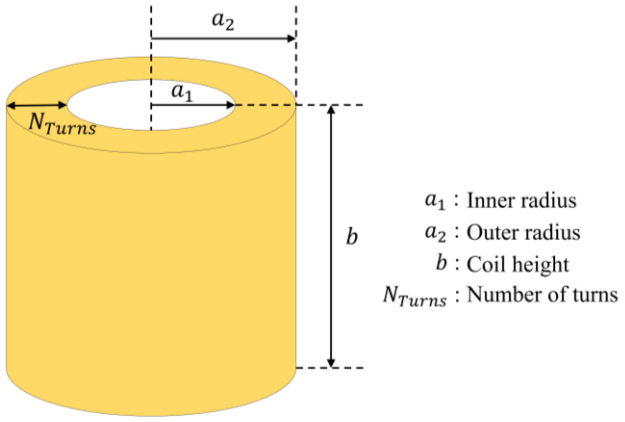

Fig. 2. Geometric illustration of SMES coil with key design parameters.

2.4. Scaling analysis of design parameters in SMES design

As the energy capacity increases, the design parameters depend on a scaling factor (k) and exhibit characteristic changes due to size dependency. Let k represent the scaling factor. The solenoidal coil's inner radius (a_1), outer radius (a_2), and height (b) scale proportionally with k, resulting in dimensions of ka_1, ka_2, and kb, respectively.

The coil's height and inner diameter increase with energy capacity because the stored energy is proportional to the coil's volume ($V \propto k^3$), requiring larger energy storage space. Similarly, the outer diameter increases due to its dependence on the cross-sectional area ($A \propto k^2$) and the number of turns ($N \propto k^2$), which allow for the inclusion of more conductor.

The current density decreases ($J \propto 1/k$) as the energy capacity increases to maintain thermal and electromagnetic stability. Table I shows this trend, with current density decreasing from 193.4 A/mm^2 at 1 MJ to 32.4 A/mm^2 at 1 GJ. Meanwhile, the operating current remains relatively consistent between 100 A and 111 A, highlighting the role of total inductance in energy scaling.

While the center field (B_z) varies between 3.8 T and 5.2 T, these fluctuations remain within a range that ensures stable performance as the energy capacity increases. According to (5), the center field scales proportionally with k, where α and β are dimensionless parameters related to the solenoidal coil's geometry. These parameters represent the winding outer diameter and coil height, normalized to the winding inner diameter [16].

$$\mathrm{B_z}(0,0) = \frac{\mu_0 NI}{2a_1(\alpha-1)} \ln\left(\frac{\alpha+\sqrt{\alpha^2+\beta^2}}{1+\sqrt{1+\beta^2}}\right) \propto k \tag{5}$$

The increase in energy capacity significantly affects the total inductance, as shown in (6). Table I demonstrates that total inductance increases from 162.8 H at 1 MJ to 181,635 H at 1 GJ, underscoring its importance in stored energy calculations. The relationship $L \propto k^5$ aligns with this trend, highlighting the need for precise inductance design to accommodate higher energy capacities.

$$\mathrm{E} = \frac{1}{2}\frac{B^2}{\mu_0} V \propto k^5 ; \quad \mathrm{L} = \frac{2\mathrm{E}}{(I_{op})^2} \propto k^5 \tag{6}$$

This scaling analysis highlights that key design parameters, including volume, current density, and total inductance, adjust proportionally to ensure the SMES coil can achieve higher energy capacities while maintaining stability and efficiency.

3. COST ANALYSIS OF HTS CONDUCTOR FOR SMES DESIGN

3.1. Significance of the HTS conductor in SMES design

The key components of the SMES system are the power conditioning system (PCS) for AC/DC bidirectional power conversion, the cryogenic system for cooling the SMES coil, and the superconducting coil made of HTS conductor. The term "HTS conductor" broadly refers to HTS tape, and the two are used interchangeably in this context. Among

these components, HTS conductor plays a significant role in the overall system design.

While the cryogenic system and PCS also contribute to the total cost of the SMES system, the extensive length of HTS tape is one of the primary cost factors. This is due to the high material cost of HTS tape and the current challenges associated with its mass production. Therefore, analyzing the cost of HTS tape is essential when designing SMES systems for various energy capacities.

The extensive length of HTS tape in high-capacity SMES designs, such as the 1 GJ SMES, may require multiple joints, which could act as heating sources and pose thermal management challenges. However, this research focuses solely on the material cost and production challenges associated with the HTS tape, excluding the contributions of the cryogenic system, PCS, or joint-related effects.

3.2. Calculation of estimated costs for HTS conductor

The HTS tape used for the SMES coil design in this research is a SuNAM REBCO tape with a minimum critical current of 200 A. The approximate unit cost of the selected HTS tape is $20 per meter. The total conductor length for various energy capacities, ranging from 1 MJ to 1 GJ as shown in Table I, is multiplied by the unit cost of the HTS tape. The resulting costs for HTS tape that meet the required energy capacities are summarized in Table II.

In Table II, the first row shows the required length of HTS tape, measured in kilometers, for each energy capacity. The second and third rows show the calculated costs of HTS conductor in thousand US dollars (USD) and billion South Korean won (KRW), respectively. The last row represents the energy unit cost in USD per joule, calculated by dividing the cost of HTS tape for each energy capacity by the corresponding stored energy.

For instance, the energy unit cost of $1.10/J in the 1 MJ column is calculated by dividing 1,102 thousand USD by 1 million joules.

Fig. 3 visualizes the energy unit cost as a function of energy capacities ranging from 1 MJ to 1 GJ. The graph shows that the energy unit cost of the HTS conductor decreases as the total length of HTS tape and the energy capacity increase. This downward trend suggests that large-scale HTS SMES designs require thousands of kilometers of HTS conductor. However, the actual cost is expected to remain relatively low, supporting the feasibility of designing and constructing HTS SMES systems with energy capacities beyond 1 GJ. Thus, the overall cost efficiency improves, making large-scale HTS SMES systems more economically viable.

3.3. Economic implications of HTS conductor

Building on the declining trend of energy unit cost shown in Fig. 3, further reductions in the overall cost of the HTS SMES system are feasible through the establishment of a mass production system for HTS tape and improvements in manufacturing capabilities [17].

According to Table II, the mass production of GdBCO HTS tape could reduce the overall cost of HTS SMES by enabling the fabrication of longer HTS tapes. The feasibility of mass production could support the development

TABLE II
COSTS OF HTS CONDUCTOR AND ENERGY UNIT COST.

	1 MJ	5 MJ	10 MJ	50 MJ	100 MJ	500 MJ	1 GJ
Coil Length (km)	55.1	146.3	223.2	684.9	828.5	2,685.9	3,729.1
Cost (Thousand USD)	1,102	2,926	4,464	13,698	16,570	53,718	74,582
Cost (Billion KRW)	1.6	4.1	6.3	19.4	23.5	76.1	105.6
Energy Unit Cost ($/J)	1.10	0.59	0.45	0.27	0.17	0.11	0.075

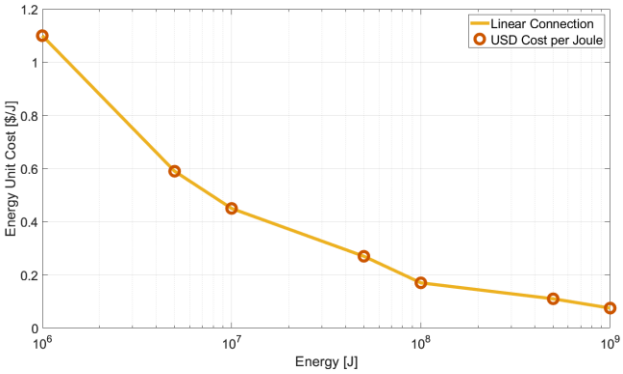

Fig. 3. Visualization of the energy unit cost as a function of the energy capacities.

of larger-scale SMES systems. As demand for these systems grows, production efficiency is likely to improve, further driving down costs.

4. CONCLUSION

This study focuses on energy capacities from 1 MJ to 1 GJ, alongside a detailed cost analysis of the HTS conductor central to their design. By applying FEM-based parametric sweep processes, key design parameters such as conductor length, operating current, inductance, and center magnetic field were evaluated across various energy capacities to ensure system efficiency and stability.

The cost analysis revealed that HTS tape, as one of the predominant cost drivers in SMES systems, significantly influences the overall system cost. The calculated energy unit cost ($/J) showed a decreasing trend as energy capacity increased. Moreover, the potential for further cost reductions through the mass production of HTS tape underscores the feasibility of large-scale SMES implementation.

These findings highlight the transformative potential of HTS SMES in modern energy storage, addressing critical challenges in power grid stabilization and renewable energy integration through high energy density and operational efficiency. The feasibility of cost reduction, particularly in HTS tape production, supports the long-term economic viability of these systems, positioning HTS SMES as a promising technology for future industrial adoption and the development of sustainable energy infrastructures.

Future research should extend beyond HTS tape to include integrated SMES systems that account for power conditioning systems, cryogenic systems, and other control systems. Performing cost analyses on such integrated systems would provide a more comprehensive understanding of SMES system economics. Furthermore, applying these findings to real-world power systems and

industrial infrastructures could address operational and economic needs, such as dynamic load balancing and energy reliability. This research product will advance the feasibility of SMES systems, expand their applications, and reinforce their potential as a keystone of future energy storage solutions.

ACKNOWLEDGMENT

This work was supported by the Technology Innovation Program (RS-2024-00419081, Development of a high-voltage (6.9kV)/large-capacity (10MVAR) Press-Pack IGBT applied voltage converter system for supplying voltage sources to power grid) funded by the Ministry of Trade, Industry & Energy (MOTIE, Korea).

REFERENCES

[1] C. K. Das, O. Bass, G. Kothapalli, T. S. Mahmoud, and D. Habibi, "Overview of energy storage systems in distribution networks: Placement, sizing, operation, and power quality," *Renew. Sust. Energ. Rev.*, vol. 91, pp. 1205-1230, 2018.

[2] J. Zhu, H. Zhang, W. Yuan, M. Zhang, and X. Lai, "Design and cost estimation of superconducting magnetic energy storage (SMES) systems for power grids," *2013 IEEE PES Gen. Meeting*, pp. 1-5, 2013.

[3] W. Yuan *et al*., "Design and Test of a Superconducting Magnetic Energy Storage (SMES) Coil," *IEEE Trans. Appl. Supercond*., vol. 20, no. 3, pp. 1379-1382, 2010.

[4] S. M. Schoenung, W. R. Meier, and R. L. Bieri, "Small SMES technology and cost reduction estimates," *IEEE Trans. Energy Convers.*, vol. 9, no. 2, pp. 231-237, 1994.

[5] A. Molodyk and D. C. Larbalestier, "The prospects of high-temperature superconductor," *Science*, vol. 380, no. 6651, pp. 1220-1222, 2023.

[6] D. G. Whyte, et al., "Smaller & Sooner: Exploiting High Magnetic Fields from New Superconductor for a More Attractive Fusion Energy Development Path," *J. Fusion Energy*, vol. 35, pp. 41-53, 2016.

[7] S. M. Schoenung, et al., "Design, performance, and cost characteristics of high temperature superconducting magnetic energy storage," *IEEE Trans. Energy Convers.*, vol. 8, no. 1, pp. 33-39, 1993.

[8] U. Bhunia, S. Saha, and A. Chakrabarti, "Design optimization of superconducting magnetic energy storage coil," *Physica C*, vol. 500, pp. 25-32, 2014.

[9] K. Yoshida, et al., "Proposals for the final design of the ITER central solenoid," *IEEE Trans. Appl. Supercond*., vol. 14, no. 2, pp. 1405-1409, 2004.

[10] M. J. Dedicatoria, H. S. Shin, H. S. Ha, S. S. Oh, and S. H. Moon, "Electro-mechanical Property Evaluation of REBCO Coated Conductor Tape with Stainless Steel Substrate," *Prog. Supercond. Cryog.*, vol. 12, no. 4, pp. 20-23, 2010.

[11] S. Awaji, et al., "Superconducting and Mechanical Properties of Impregnated REBCO Pancake Coils Under Large Hoop Stress," *IEEE Trans. Appl. Supercond.*, vol. 23, no. 3, pp. 4600305-4600309, 2013.

[12] T. Watanabe, et al., "Strengthening Effect of "Yoroi-Coil Structure" Against Electromagnetic Force," *IEEE Trans. Appl. Supercond.*, vol. 25, no. 3, pp. 8400204-8400207, 2015.

[13] W. D. Markiewicz, M. R. Vaghar, I. R. Dixon, and H. Garmestani, "Generalized plane strain analysis of solenoid magnets," *IEEE Trans. Magn.*, vol. 30, no. 4, pp. 2233-2236, 1994.

[14] A. W. Zimmermann and S. M. Sharkh, "Design of a 1 MJ/100 kW high temperature superconducting magnet for energy storage," *Energy Rep*., vol. 6, no. 5, pp. 180-188, 2020.

[15] S. Hahn, D. K. Park, J. Bascunan, and Y. Iwasa, "HTS Pancake Coils Without Turn-to-Turn Insulation," *IEEE Trans. Appl. Supercond*., vol. 21, no. 3, pp. 1592-1595, 2011.

[16] Y. Iwasa, "Case Studies in Superconducting Magnets: Design and Operational Issues," *Springer*, US, 2009.

[17] H. Kumakura, "Development and Prospects for the Future of Superconducting Wires," *Jpn. J. Appl. Phys.*, vol. 51, no. 1R, pp. 1-6, 2011.